
Feature-Based and Output-Based Grid Adaptation Study for Hypersonic Propulsive Deceleration Jet Flows

Hicham Alkandry¹, Michael A. Park², William L. Kleb³, and Iain D. Boyd⁴

¹ University of Michigan, halkandr@umich.edu

² NASA LaRC, Computational AeroSciences Branch, Mike.Park@NASA.gov

³ NASA LaRC, Aerothermodynamics Branch, Bill.Kleb@NASA.gov

⁴ University of Michigan, iainboyd@umich.edu

1 Introduction

The size requirements for conventional aerodynamic decelerators (parachutes) used to slow Mars entry vehicles during atmospheric descent are becoming unfeasible due to the increasing mass and landing site altitude of future missions. One alternative is propulsive decelerator (PD) jets. The use of PD jets, however, involves complex flow interactions that are still not well understood. Computational fluid dynamics (CFD) is currently being investigated as a tool for predicting these flow interactions. However, manually generating appropriate grids for these flows is difficult and time consuming because of the complexity of the flowfield. Therefore, automatic grid adaptation techniques present an attractive option to accurately capture the flow features and interactions. This study compares the grids and solutions for hypersonic PD jet flows using feature-based and output-based grid adaptation techniques.

2 Numerical Setup and Approach

The present study uses a scaled-down Mars Science Laboratory (MSL) aeroshell with a single-nozzle sonic PD jet located at the center of the forebody [1]. The freestream Mach number is 12, and the thrust coefficient of the PD nozzle, defined as the thrust force normalized by the product of the freestream dynamic pressure and the aeroshell frontal area, is 0.5. The Reynolds numbers for the freestream (based on the diameter of the aeroshell) and the PD jet (based on the diameter of the nozzle-exit) are both roughly equal to 1,200, which suggests that both flows are laminar.

The numerical simulations are carried out using FUN3D (<http://fun3d.larc.nasa.gov>). FUN3D is a suite of codes predominately developed at NASA Langley that includes a 3-D Navier-Stokes equations solver for compressible flows.

The solver uses the finite-volume method on unstructured grids to solve the set of partial differential equations. For this study, time integration is performed with a point-implicit method. FUN3D also has feature-based and output-based grid adaptation capabilities that include parallel 3-D grid mechanics such as enrichment, coarsening, and element connectivity [4, 5].

The feature-based adaptation in FUN3D targets local errors in the solution due to gradients of a specific flow variable [2]. For this study, the isotropic mesh density metric is given by the first derivative of the Mach number; and the anisotropic orientation and scaling metrics are computed by the second derivative tensor (i.e. Hessian) of the Mach number. The output-based (i.e. adjoint-based) grid adaptation method in FUN3D is a 3-D extension of the methods of Venditti and Darmofal [6] that adapts the mesh to reduce the simulation error in an output functional [3], axial force on the vehicle in this case. The anisotropic metric is determined by a combination of the embedded-grid error estimation procedure and the Mach Hessian.

3 Results

Figure 1 shows the mesh and Mach number contours on the plane of symmetry for the initial, unadapted, grid. The mesh in Figure 1(a) includes an anisotropic region near the surface of the aeroshell to accurately capture the flow in the boundary layer. For the present study, this region is frozen and only the mesh outside this layer can be adapted automatically due to limitations in the current grid adaptation mechanics. The Mach number contours in Figure 1(b) illustrate the complex flow features that are generated due to the PD jet. The figure also shows that these features are not adequately captured due to coarse and misaligned elements in the initial grid.

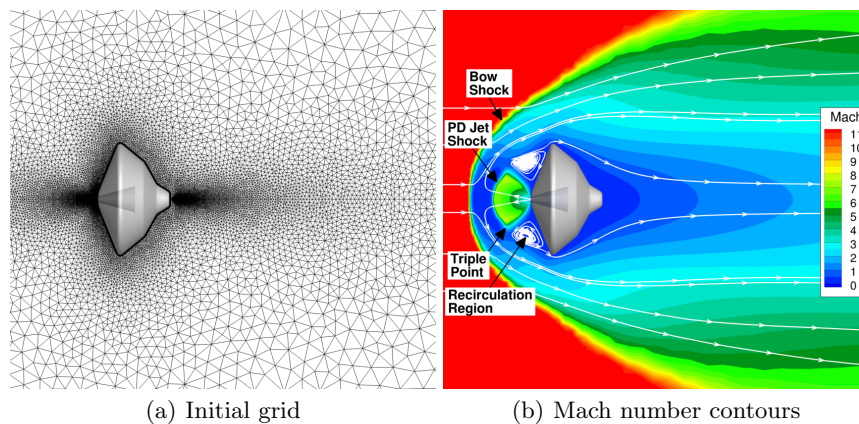


Fig. 1. Initial grid and solution.

Table 1 provides the size of the initial and adapted grids. The final adaptation cycle is determined by examining the convergence of the axial force coefficient (i.e. axial force normalized by the product of the freestream dynamic pressure and aeroshell frontal area) of the aeroshell, shown in Figure 2, and limitations in available computational resources. The feature-based method roughly doubles the number of nodes after each cycle and adds more points per cycle compared to the output-based method. The feature-based method inserts new nodes throughout the domain where local gradients are large. The output-based method only adds points where they improve calculation of the specified functional (axial force).

Table 1. Grid size ($\times 10^6$ nodes).

	Feature-based	Output-based
Initial	0.7	0.7
1 st Cycle	1.6	1.5
2 nd Cycle	4.1	3.1
3 rd Cycle	10.2	4.3
4 th Cycle	23.7	7.7

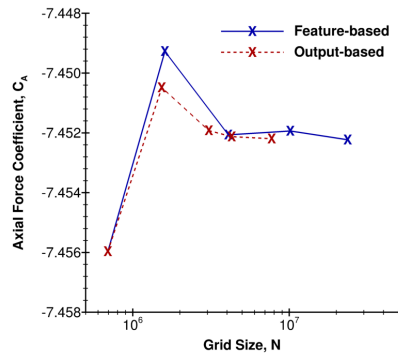


Fig. 2. Axial force coefficient.

Figure 3 shows the final adapted grids for the feature-based and output-based methods. The figure shows that the feature-based method adds more points than the output-based method near the bow shock in the wake, at the boundaries of the recirculation zone and the PD jet, and in the expansion fans that develop around the shoulders of the aeroshell. The output-based technique inserts nodes on the stagnation streamline where freestream flow and PD jet mix. This stagnation region is ignored by the feature-based technique because of relatively weak gradients in this important region.

Mach number contours on the plane of symmetry for the final adapted grids are shown in Figure 4(a). The solutions for the two grids are in overall good agreement, except in the wake where the bow shock is thicker for the output-based adapted grid due to less grid resolution. These differences in the solution, however, are inconsequential because they weakly impact the axial force of the configuration. Figure 4(b) compares the Mach number distribution along the PD jet centerline for the initial and the final adapted grids. The figure shows that the solutions for the adapted meshes are in good agreement, but the initial grid produces thicker bow and jet shocks. This result can also be seen in Figure 4(c), which shows the Mach number distribution at 0.15 aeroshell diameters away from the nozzle-exit (the dashed line in Figure 4(a))

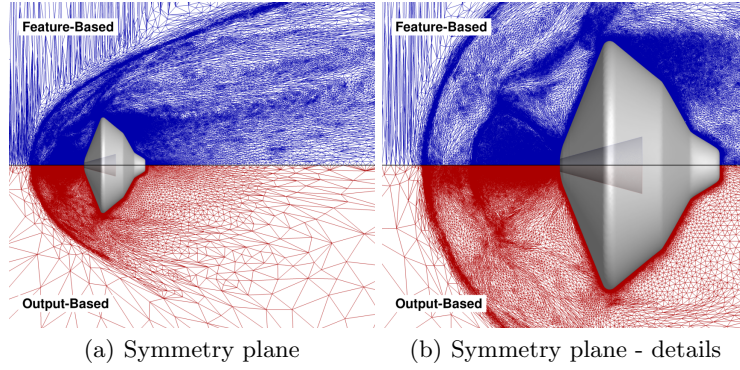
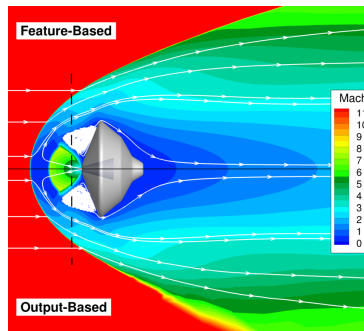
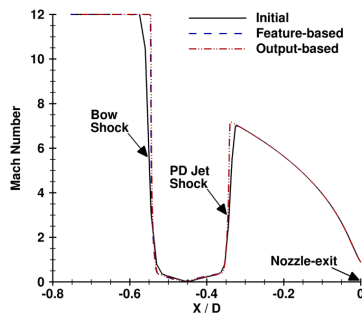


Fig. 3. Final adapted grids (top: feature-based; bottom: output-based).

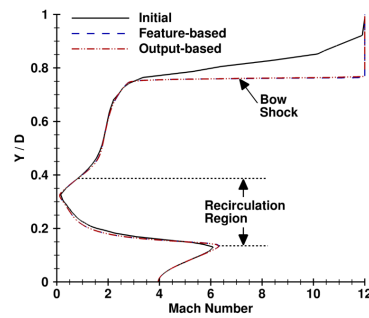
for the initial and adapted grids. Although the solutions for the two adapted grids are in overall good agreement, the feature-based adapted grid is over $3\times$ larger than the output-based adapted grid.



(a) Mach number contours



(b) Centerline



(c) $X/D = -0.15$

Fig. 4. Solution comparison.

4 Summary

This study compared the solutions and adapted meshes for a Mars entry aeroshell in Mach 12 flow with a single-nozzle sonic PD jet. The grids were adapted using feature-based and output-based methods for 3-D viscous flows. The study found that the feature-based adaptation technique roughly doubled the number of nodes in the grid after each adaptation cycle and overall added more nodes than the output-based technique. The feature-based method inserted more nodes near the bow shock in the wake, at the boundaries of the recirculation zone and the PD jet, and in the expansion fans that develop around the shoulders of the aeroshell compared to the output-based method. The solutions for these two methods were in good agreement, but the bow shock thickness in the wake was larger for the output-based adapted grid due to lower grid resolution. As a conclusion, this study found that the feature-based technique can be computationally expensive for these types of flows, especially for large computational domains with extended wake regions.

References

- [1] H. Alkandry, I. D. Boyd, E. M. Reed, J. R. Codoni, and J. C. McDaniel. Interactions of single-nozzle sonic propulsive deceleration jets on mars entry aeroshells. In *AIAA Paper 2010-4888*, June 2010.
- [2] K. L. Bibb, P. A. Gnoffo, M. A. Park, and W. T. Jones. Parallel, gradient-based anisotropic mesh adaptation for re-entry vehicle configurations. In *AIAA Paper 2006-3579*, June 2006.
- [3] M. A. Park. Adjoint-based, three-dimensional error prediction and grid adaptation. In *AIAA Paper 2002-3286*, June 2002.
- [4] M. A. Park. *Anisotropic output-based adaptation with tetrahedral cut cells for compressible flows*. PhD thesis, Massachusetts Institute of Technology, September 2008.
- [5] M. A. Park and D. L. Darmofal. Parallel anisotropic tetrahedral adaptation. In *AIAA Paper 2008-917*, January 2008.
- [6] D. A. Venditti and D. L. Darmofal. Anisotropic grid adaptation for functional outputs: application to two-dimensional viscous flows. *Journal of Computational Physics*, 187:22–46, 2003.